American Journal of Applied Chemistry
2023; 11(5): 122-129
http://www.sciencepublishinggroup.com/j/ajac
doi: 10.11648/j.ajac.20231105.12
ISSN: 2330-8753 (Print); ISSN: 2330-8745 (Online)

Synthesis of Metallic Silver Supported by Metal Oxides (Fe_2O_3 and CoO) for the Removal of Methylene Blue in the Presence of Sunlight

Donourou Diabate[1], Koffi Pierre Dit Adama N'goran[2, *], Tano Patrice Fato[2], N'Guessan Louis Berenger Kouassi[2]

[1]Laboratory of Physical Chemistry, Félix Houphouët-Boigny University, Abidjan, Côte d'Ivoire

[2]Training Research Unit of Biological Sciences, Department of Mathematic Physic and Chemistry, Peleforo Gon Coulibaly University, Korhogo, Côte d'Ivoire

Email address:

ngorankoffipierre@gmail.com (Koffi Pierre Dit Adama N'goran)

[*]Corresponding author

To cite this article:

Donourou Diabate, Koffi Pierre Dit Adama N'goran, Tano Patrice Fato, N'Guessan Louis Berenger Kouassi. Synthesis of Metallic Silver Supported by Metal Oxides (Fe_2O_3 and CoO) for the Removal of Methylene Blue in the Presence of Sunlight. *American Journal of Applied Chemistry*. Vol. 11, No. 5, 2023, pp. 122-129. doi: 10.11648/j.ajac.20231105.12

Received: August 2, 2023; **Accepted**: August 29, 2023; **Published**: October 9, 2023

Abstract: The aim of this study was to evaluate and compare the effectiveness of the combination of silver nanoparticles (Ag NPs) and two metal oxides (Fe_2O_3 and CoO) for the removal of methylene blue (MB) molecules from aqueous solutions. To achieve this purpose, Silver (Ag) nanoparticles were successfully deposited onto metal oxides (Fe_2O_3 and CoO) nanocomposites, which were employed as adsorbents and photocatalysts. The prepared photocatalysts (Ag/Fe_2O_3 and Ag/CoO) were used for the absorption of methylene blue, an organic pollutant. Various analytical techniques such as Field Emission Scanning Electron Microscope (FESEM), Energy Dispersive X-ray (EDX), and Powder X-ray diffraction (XRD) were used to characterize the prepared nanomaterials. The results of the energy dispersive X-ray analysis identified the presence of the elements (Ag, Fe, and Co) and their distribution on the surface of the material. The X-ray diffraction pattern also confirmed the formation of nanocomposites (Ag/Fe_2O_3 and Ag/CoO). The degradation of MB in the presence of sunlight ratified that the nanocomposites (Ag/Fe_2O_3 and Ag/CoO) had weak photocatalytic absorption efficiency controlled by pseudo-second order kinetic model. Comparing both nanocomposites, the nanocomposite (Ag/Fe_2O_3) showed the best photocatalytic performance with a percentage of 56% within 3h. The results of the photocatalytic experiments indicated that the introduction of Ag into the metal oxides limited the charge recombination process between the photogenerated electrons/holes and thus facilitated the absorption of methylene blue.

Keywords: Silver Nanoparticles, Nanocomposites, Photocatalytic, Metal Oxide, Pseudo- Second Order, Absorption

1. Introduction

In recent years, nanomaterials have been at the heart of nanoscience and nanotechnology. This multidisciplinary field of study is expanding rapidly, attracting considerable investment and effort in research and development around the world. Nanoporous materials, as a subset of nanostructured materials, possess unique surface, structure, and bulk properties. These features highlight their important uses in diverse conventional methods such as ion exchange, separation, catalysis, sensors, isolation, and purification of biological molecules [1-3]. Nanoporous materials have been gaining scientific and technological attention due to their faculty to interact with the surface of ions, atoms or molecules and throughout the bulk counterparts as well. [4]. Colloidal micro and nanospheres have been attracting great interest from researchers because their intrinsic properties can be finely tuned by altering parameters including diameter, chemical composition, bulk structure, and crystallinity [5]. Coating nanospheres with noble metal nanoparticles (NMNPs), oxide nanoparticles, or semiconductor quantum dots can impart

specific catalytic, magnetic, and optoelectronic properties to them. Moreover, they greatly expand their utility in numerous areas such as electronics, magnetism, optics, and catalysis [6, 7]. For example, several chemists have shown that nanosilver plays an important role in catalysis, which has been widely explored in many organic transformations up to fine chemical synthesis [8, 9]. Dispersion of AgNPs on different substrates to form various composites is one of the applicable strategies, such as Ag/(carbonaceous materials), Ag/(metal oxide), Ag/(non-metal oxide), Ag/(metal hydroxide), and Ag/(dual hydroxide material layer) [10]. In addition, the aforementioned strategies would be effective techniques to remove pestilential dyes from wastewater. These organic pollutants are present in wastewater and are arised from textile, paper, plastic, leather, food, and cosmetic industries [11]. Unfortunately, they are one of the major sources of environmental degradation of water [12]. Discharge of these wastewaters containing dyes and its derivatives can lead to human health risks, reduction of light penetration in the aquatic environment, and other environmental threats [13-15]. Thus far, several methods namely absorption [16], hydrogenation [17], photocatalysis [18-22], biodegradation [23], and chemical oxidation [24, 25] have already been applied in the remediation of these industrial wastewaters prior to their release to the environment. Herein, we reported a facile green synthesis method for the preparation of heterostructure Ag coated metal oxides and successfully used as adsorbents and photocatalysts for the removal of MB from contaminated water [26, 27]. For this purpose, we first prepared a carbon sphere under hydrothermal conditions from glucose and porous metal oxides. The monodisperse colloidal nanospheres were obtained in an aqueous glucose solution and no toxic reagents were used. The objective of this work is to propose new alternative metal oxides such as Fe_2O_3 and CoO coupled with Ag for methylene blue degradation. Thus, to evaluate the efficiency of the catalysts (Ag/Fe_2O_3 and Ag/CoO), a comparative study between both nanocomposites for the removal of methylene blue from an aqueous solution has been performed.

2. Experimental Section

2.1. Materials

2.1.1. Reagents

The following reagents were required for this experiment. Silver nitrate ($AgNO_3$), Iron (III) nitrate nonahydrate ($Fe(NO_3)_3.9H_2O$), and Cobalt (II) nitrate hexahydrate ($Co(NO_3)_3.6H_2O$) were purchased from New Delhi (India). Methylene blue was supplied by the reagent factory in New Delhi, India. Polyvinylpyrrolidone (PVP) was obtained from Sigma-Aldrich (India). All other solvents and reagents used were purified by standard methods.

2.1.2. Apparatus

The morphologies of the samples obtained (Porous Metal Oxides (PMO), catalysts) were examined with Field Emission Scanning Electron Microscope (FESEM, FEI Nova-Nano SEM-600, Netherlands) and elemental composition was investigated through the same instrument using the energy dispersive X-ray analysis (EDX). Powder X-ray diffraction (XRD) patterns were measured by using RICH-SIEFERT 3000-TT diffractometer employing Cu K_α radiation. The used spectra were recorded on a double beam spectrophotometer (Shimadzu UV-1208 model, Japan).

2.2. Synthesis Procedure

2.2.1. Synthesis of Metal Silver Nanoparticles

Silver nanoparticles (AgNPs) were fabricated basing on previous reported method [28]. The description of this method consists of adding 0.5 g of PVP into 60 mL of a methyl alcohol and stirred firmly. Afterwards, 1 g of $AgNO_3$ was also added into the obtained mixture. After stirring, the solution was transferred to a 100 mL autoclave and heated to 200 °C for 24 h. The resulting precipitate was carefully rinsed thoroughly and dried at 80 °C for 4h. The final powder was Ag.

2.2.2. Synthesis of Carbon Spheres

Carbon spheres were prepared by hydrothermal method. In this procedure, 3g of glucose were dissolved in 17 mL of water to form a clear solution. The solution was placed in a 20 mL Teflon-lined sealed stainless-steel container and heated at 180°C for 3 h. The solid brown product was isolated and purified by repeated washing with water and ethanol. And then, it dried at 80°C for 4 h. The as-prepared carbon spheres along with PVP were used as templates to synthesize the porous metal oxides [29].

2.2.3. Synthetic Procedure for Porous Metal Oxides

In a typical synthesis, 0.5 g of $M(NO_3)_x$ (where M = Co and Fe; x=2) was dissolved in 20 mL of 1: 1 (V/V) water and ethanol mixture. To this solution, 1 g polyvinylpyrrolidone polymer and 50 mg of the as-prepared carbon spheres were added and mixed thoroughly to make homogeneous viscous slurry. The obtained slurry was then poured into a glass petri dish (50 mm diameter) and aged for 10 h in an oven at 80°C. The transparent film of $M(NO_3)_x$. PVP composite thus obtained was calcined at 550°C for duration of 5 h with a heating rate of 1°C min^{-1}. The sample was cooled to room temperature at a rate of 3°C min^{-1} [29].

2.2.4. Synthesis of Catalysts Supported on Porous Metal Oxides (PMO)

$AgNO_3$ and the above obtained PMO (CoO and Fe_2O_3) with a mass ratio of Ag to (Ag + PMO) = 10 wt% were mixed thoroughly in de-ionized water. $NaBH_4$ aqueous solution was added drop wise to the obtained mixture. A sonication step of 5 min is performed just before a constant mechanical stirring for 2 h. Then, the precipitate was filtered, dried, and fired at 500°C for 5 h. The obtained sample was Ag/PMO (Ag/CoO and Ag/Fe_2O_3) [28].

2.3. Photocatalytic Setup

The photocatalytic degradation of methylene blue was evaluated with the as-synthesis Ag/PMO nanoparticles. All

the experiments were performed outdoor with sun as the main source of light. The working solution used to investigate the degradation process of MB was adjusted at 5 ppm. Then, 25 mg of the powdered phase of Ag/CoO and Ag/Fe_2O_3 were added to 10 mL of the aqueous solution of MB, individually. The obtained mixture was held in a dark closed box for 2 h before light irradiation in order to reach the adsorption equilibrium. The air was bubbled throughout the reaction to ensure the mixing of photocatalyst with dye during the photocatalytic experiment. The degradation of MB process was carried out at room temperature (25°C). The degradation efficiency (R%) was estimated via the expression as follows [30]:

$$R(\%) = \frac{C_o - C_t}{C_o} \times 100 \quad (1)$$

where C_o and C_t are the starting and the final concentration at a time (t).

3. Results and Discussion

3.1. Field Emission Scanning Electron Microscopy (FESEM) Analysis of Nanocomposite

The FESEM images with corresponding EDX spectrum for the nanocomposites (Ag/Fe_2O_3 and Ag/CoO) are shown in Figure 1. The EDX analysis revealed the presence of Ag, Fe, and O in the Ag/Fe_2O_3 nanocomposite (Figure 1C). Likewise, Ag, Co, and O were found in the Ag/CoO nanocomposite (Figure 1D). The silver peaks that appeared in the EDX spectra of the nanocomposites (Ag/Fe_2O_3 and Ag/CoO) indicated Ag was deposited on the surface of metal oxides (Fe_2O_3 and CoO). The formation of the heterostructures can be clearly seen in the FESEM images showing a very large condensation of the nanoparticles (Figure 1A' and Figure 1B') compared to the pure metal oxide nanoparticles (Figure 1A and Figure 1B).

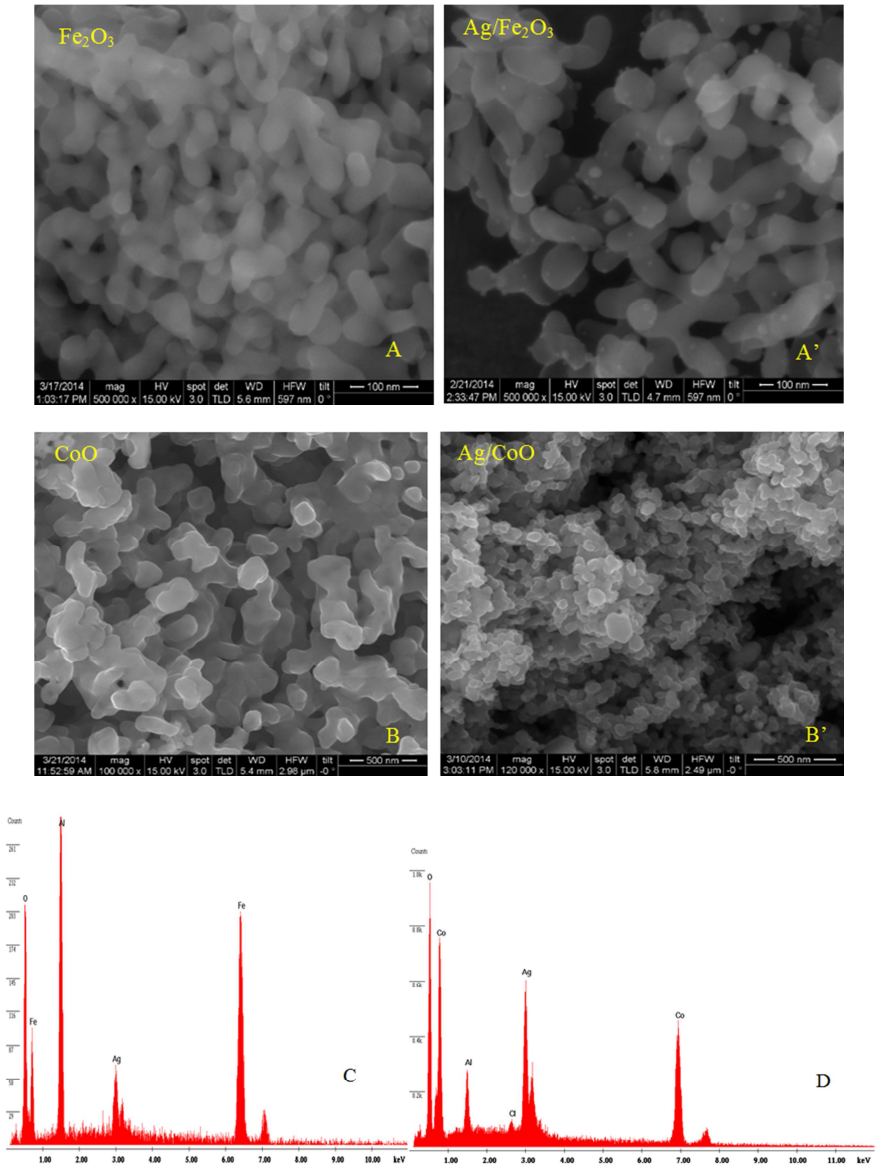

Figure 1. *FESEM micrographs of pure metal oxides Fe_2O_3 (A), CoO (B), and aggregated nanocomposites Ag/Fe_2O_3 (A') and Ag/CoO (B'). EDX spectrum for Ag/Fe_2O_3(C), Ag/CoO (D).*

3.2. X-ray Diffraction Patterns Analysis of Metal Silver and Metal Oxide Nanocomposite

The XRD patterns of bare metal silver, pure metal oxides (CoO and Fe_2O_3), and Ag/metal oxide nanocomposites (Ag/CoO and Ag/Fe_2O_3) were examined in the 2θ range of 10-80° and are shown in Figure 2. Five Ag diffraction peaks with 2θ observed at 24.79°, 38.12°, 44.34°, 64.47°, and 77.33° were assigned to (210), (111), (220), (311), and (400), respectively (ICDD 893722) (Figure 2A). All of the Fe_2O_3 diffraction peaks were attributed to the Fe_2O_3 alpha phase (JCPDs map 33-0664). Thus, Fe_2O_3 showed diffraction patterns at 24.08°, 33.17°, 35.52°, 41.02°, 49.57°, 54.14°, 62.59°, 64.25° corresponding to hkl values of (012), (104), (110), (113), (024), (116), (018), (214), (300), respectively (Figure 2B). Nevertheless, the XRD patterns of the Ag/Fe_2O_3 nanocomposite showed additional peaks at 24.11° and 64.10° corresponding to (210) and (220) planes of silver, respectively (Figure 2B'). This observation denotes the successful coating of Ag onto Fe_2O_3. Figure 2C presents main peaks of CoO at 36.82°, 44.80° and 65.25°, which were indexed to (111), (200), and (220) crystalline planes of the face-centered cubic structure of CoO nanoparticles [31-33]. In the XRD pattern of the Ag/CoO nanocomposite, in addition to the diffraction peaks of CoO, diffraction peaks of the (220) and (400) planes of silver located at 2θ values equivalent to 44.85° and 77.61° were observed, demonstrating the successful coating of silver by CoO (Figure 2C').

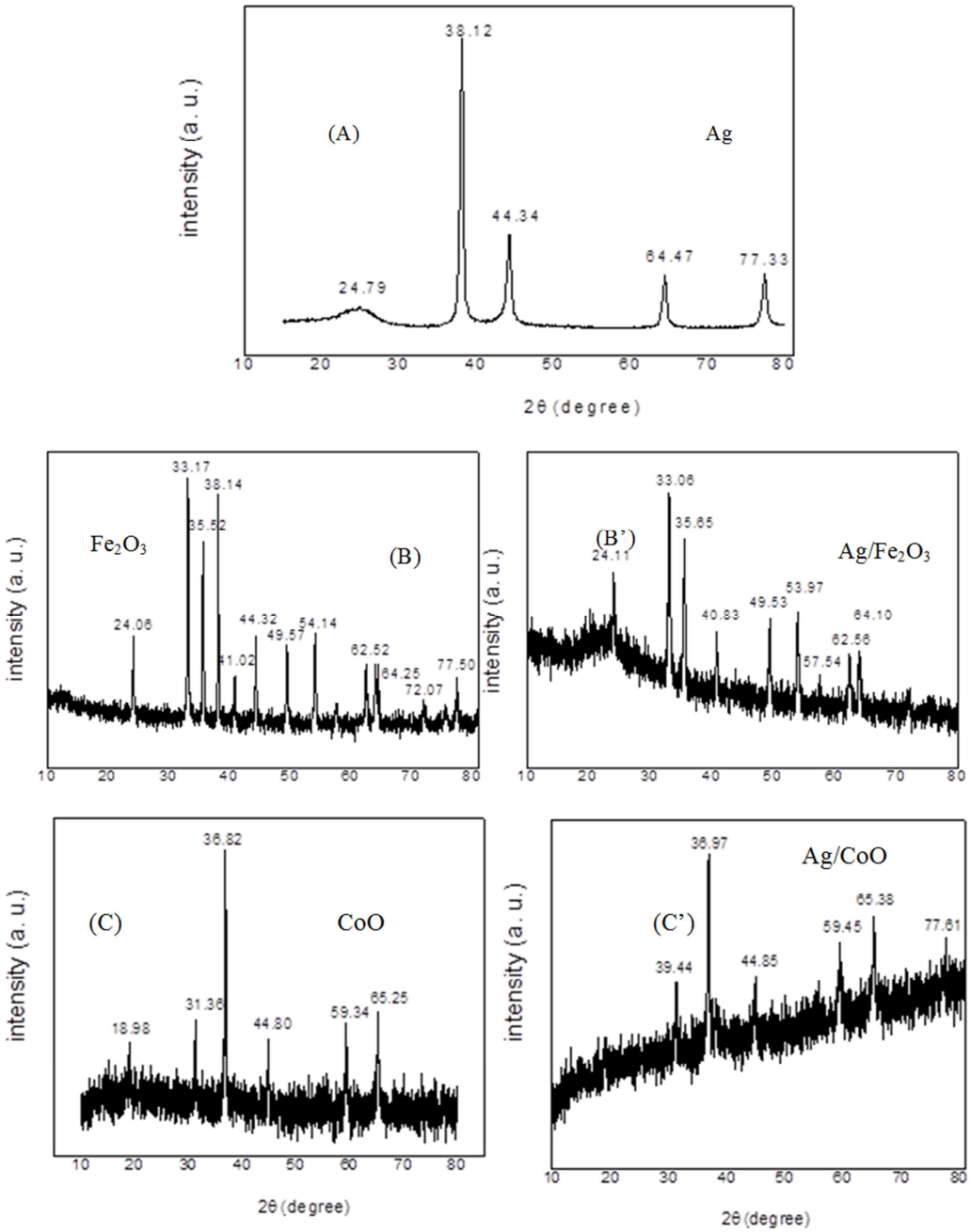

Figure 2. *X-ray diffraction patterns of the pristine, Ag (A), Fe_2O_3 (B), CoO (C), and oxide nanocomposites Ag/Fe_2O_3 (B'), Ag/CoO (C').*

4. Degradation of MB Pollutants

The photocatalytic response of the synthesized Ag/metal oxide nanocomposites were examined by methylene blue (MB) degradation. The removal process of MB was carried out with the help of sunlight. The results of the MB degradation are shown in Figure 3A. In the degradation analysis, the y-axis was plotted by C_0/ C_t, where C_t is the intensity of the absorption peak at any time and C_0 is the intensity of the initial absorption peak. The x-axis was plotted with the irradiation time of the reaction solution. The elimination of MB dye was monitored up to 3 h with constant sampling intervals in the first 20 min and then gradually reached equilibrium for the Ag/Fe_2O_3 and Ag/CoO nanocomposites (Figure 3A). As can be observed, the absorption peak gradually decreased overtime using both Ag/metal oxide nanocomposites [34]. The maximum degradation rate of methylene blue was reached 56% for the Ag/Fe_2O_3 nanocomposite in 160 min while Ag/CoO nanocomposite degraded 40% of methylene blue in 180 min (Figure 3B). Among two Ag/metal oxide nanocomposites, Ag/Fe_2O_3 had effective performance with respect to degradation time at MB.

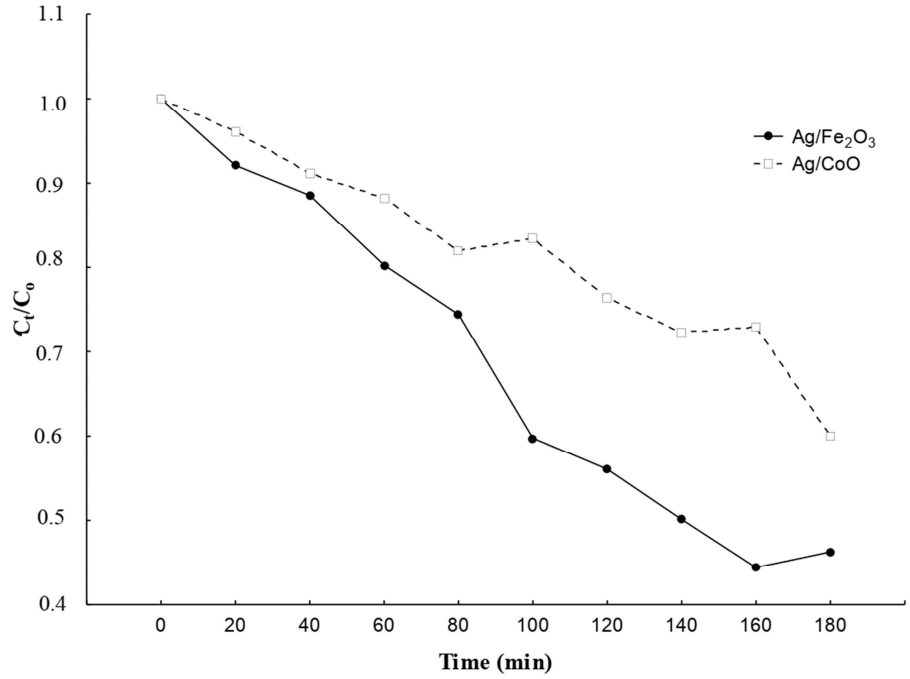

(A)

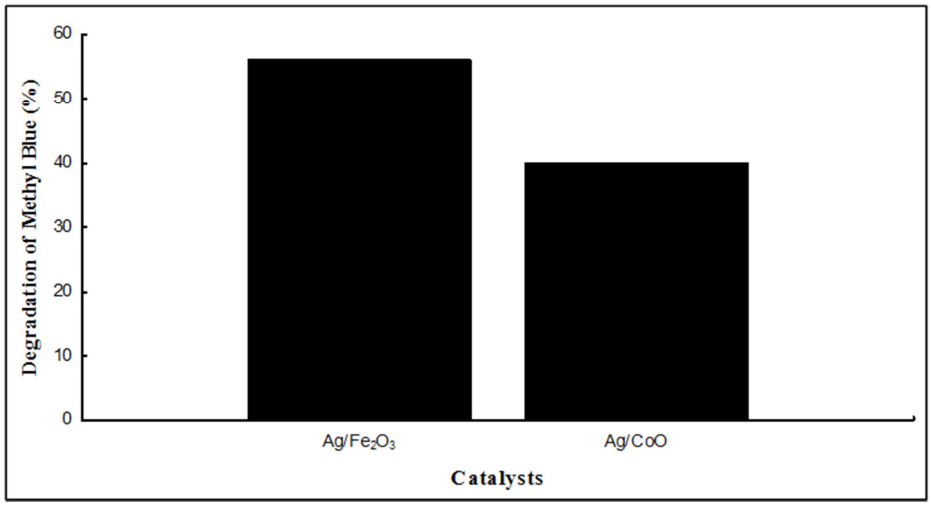

(B)

Figure 3. *(A) Time dependent degradation process of methylene blue with both nanocomposites. C_t is absorption peak intensity at any time and C_0 designates initial absorption peak intensity. (B) Comparison of photocatalytic activity between both nanocomposites (Ag/Fe_2O_3 and Ag/CoO).*

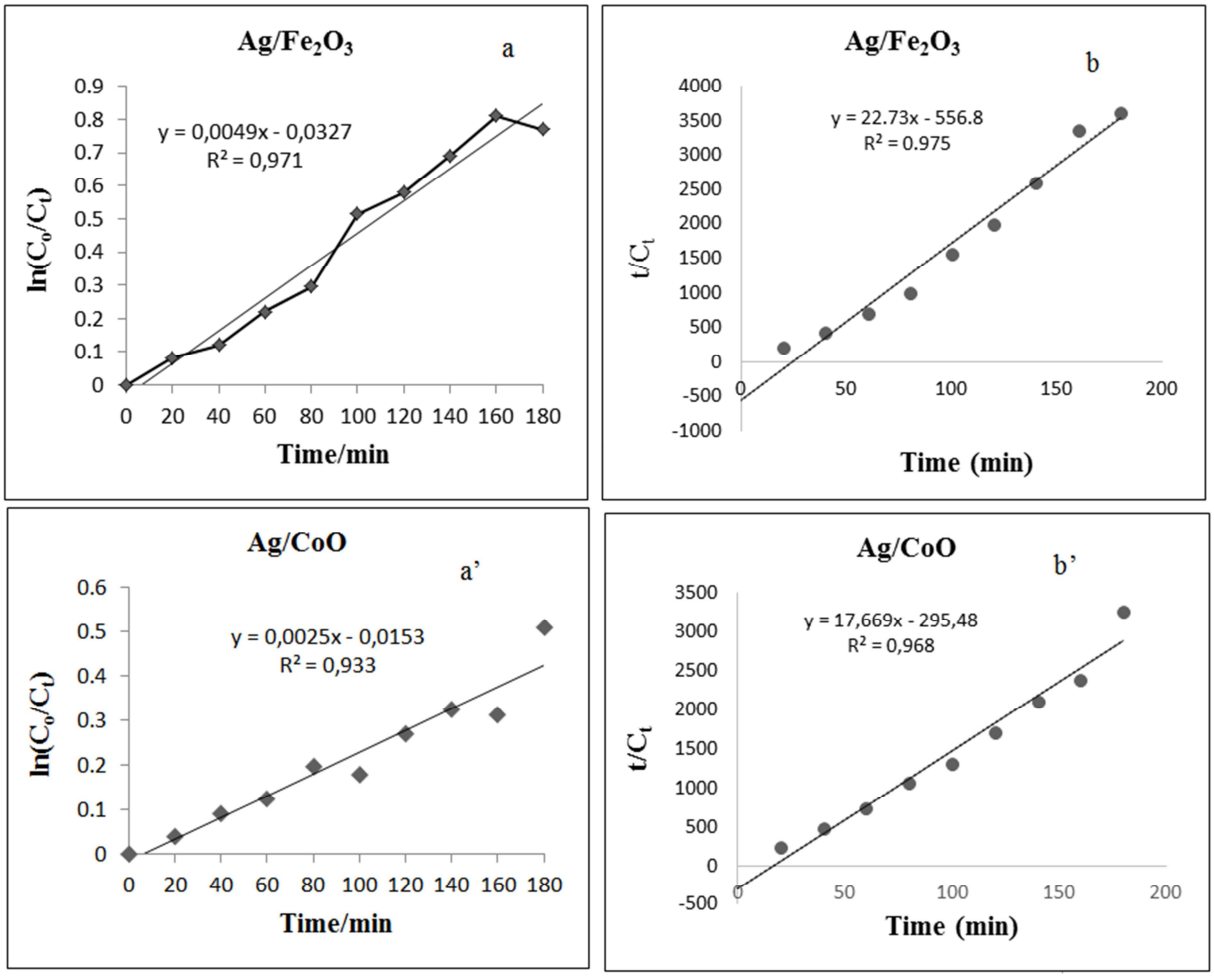

Figure 4. *Kinetic models for the adsorption of MB onto Ag/Fe_2O_3 and Ag/CoO calculated using (a) and (a') pseudo first-order kinetic models and (b) and (b') pseudo second-order kinetic models.*

The reason for the absorption capacity of Ag/Fe_2O_3 nanocomposite would be due to the surface area and pore volume the metals oxide (Table 2). Due to the pore volume and surface area the metals oxide, Ag/Fe_2O_3 was better than Ag/CoO.

Table 1. *Pseudo first-order model and pseudo second-order model parameters constant for the adsorption of MB on (Ag/Fe_2O_3 and Ag/CoO) nanocomposites.*

Adsorbents	**Methylene Blue**			
	Pseudo-first-order kinetic model		**Pseudo-second-order kinetic model**	
	k_1 (min^{-1})	**R^2**	**k_2 ($g\ mg^{-1}\ min^{-1}$)**	**R^2**
Ag/Fe_2O_3	0.0049	0.971	22.73	0.975
Ag/CoO	0.0025	0.933	17.70	0.968

The study of the absorption kinetics is one of the main characteristics showing the efficiency of the adsorbent. In addition, it allows describing the rate of solute absorption by controlling the diffusion process, the residence time of the adsorbate at the solid/solution interface and the order of the reaction [35]. To evaluate the nature of absorption mechanism and efficiency of the prepared nanocomposites (Ag/Fe_2O_3 and Ag/CoO), the most common kinetic models such as pseudo-first order and pseudo-second order were used to analyse the experimental results. The absorption kinetic studies of MB on Ag/Fe_2O_3 and Ag/CoO nanocomposites with time were then investigated by applied pseudo first-order and pseudo second-order kinetic models.

The pseudo first-order kinetic and pseudo second-order kinetic models can be expressed by the equations (2) and (3), respectively:

$$\ln\left(\frac{C_0}{C_t}\right) = k_1 t \quad (2)$$

$$\frac{1}{C_t} - \frac{1}{C_0} = k_2 t \quad (3)$$

where C_t and C_0 are the MB concentration at time t = t and t = 0, respectively, k_1 and k_2 are the pseudo first-order rate constant and the pseudo second-order rate constant, respectively. The pseudo first-order rate constant k_1 and k_2 were determined by calculating the gradient of graph ln

(C_0/C_t) against time (t) and t/C_t against time (t), respectively. From Table 1, the pseudo second-order model is much better to represent the absorption of MB by Ag/metal oxide nanocomposites, with correlation coefficients (R^2) very close to 1. This observation indicates that the MB absorption process by nanocomposites (Ag/Fe_2O_3 and Ag/CoO) was controlled by chemisorption [35].

Table 2. *Physical Properties of Metal Oxide (Fe_2O_3 and CoO).*

Oxides	Surface area (m^2/g)	Pore volume (cc/g)
CoO	23.01	0.05
Fe_2O_3	37.25	0.25

5. Mechanism for Photocatalytic Degradation of Methylene Blue

The procedure for photocatalytic degradation of methylene blue was carried out as follows. When the sunlight fell on the aqueous solution of methylene blue and photocatalysts, a series of chemical reactions was initiated leading to degradation products. Those products were comparatively less hazardous to the ecosystem [36]. The plausible mechanism of the photocatalytic degradation was postulated, where the formation of the interface between Ag and PMO (CoO and Fe_2O_3). As such, when the photocatalysts (Ag/CoO and Ag/Fe_2O_3) were irradiated by the sunlight, the electrons transit from the valence band (VB) to the conduction band (CB) of CoO or Fe_2O_3. Moreover, those electrons photogenerated in the CB of CoO or Fe_2O_3 were taken up by Ag. This phenomenon reduced the oxygen in the atmosphere and produced the superoxide radical (O^{2-}) [34]. Meanwhile, the created holes in the conduction band of CoO and Fe_2O_3 were reacted with the surface water and oxidized it to the hydroxyl radical (OH^-). Furthermore, these reactive radical intermediates were reacted with the aqueous dye solution of methylene blue and mineralized into colorless species (CO_2 and H_2O) [34, 36]. Thus, the photocatalysts (Ag/CoO and Ag/Fe_2O_3) provided an interface and a large surface area producing oxygen vacuoles and oxygen vacancy plasmonic ions. In addition, the plasmonic effect of silver itself allowed the nanocomposites (Ag/CoO and Ag/Fe_2O_3) as efficient photocatalysts.

6. Conclusion

In summary, using sunlight to study the degradation of methylene blue (MB), new photocatalyst adsorbents (i e., Ag/Fe_2O_3 and Ag/CoO) were successfully synthesized and characterized by FESEM, XRD, and EDX. The XRD pattern confirmed the presence of Ag on the metal oxides (Fe_2O_3 and CoO). The kinetic process was successfully fitted to pseudo-second order kinetic models. The fabricated nanocomposites namely Ag/Fe_2O_3 and Ag/CoO showed low photocatalytic absorption of MB with respective percentages of 56% and 40%. This degradation of methylene blue would be due to the strong interfacial interactions between Ag and metal oxides (Fe_2O_3 and CoO) that allowed the creation of oxygen vacuoles and oxygen vacuole plasmonic ions. In addition, the superoxide radical (O^{2-}) is the main intermediate responsible for the degradation of methylene blue (MB).

Declaration of Competing Interest

All authors have read the manuscript, agree with the journal's data deposition requirements and to our submission in Catalysis today, and have no conflicts of interest.

Author Statement

Author contribution: Koffi Pierre Dit Adama N'goran: Conceptualization, data curation, formal analysis, investigation, methodology, validation, writing-original draft, and editing. N'guessan Louis Berenger Kouassi: Conceptualization, data curation, formal analysis, investigation, methodology, supervision, validation, writing-original draft, and editing. Donourou Diabate: Conceptualization, data curation, formal analysis, investigation, methodology, supervision, validation, writing-original draft, and editing. Tano Patrice Fato: Conceptualization, data curation, formal analysis, investigation, methodology, validation, writing-original draft, and editing.

References

[1] N. Baig, I. Kammakakam, W. Falath, Nanomaterials: a review of synthesis methods, properties, recent progress, and challenges. Materials Advances. 2 (6) (2021)1821-1871.

[2] Y. He, Z. Wang, H. Wang, Z. Wang, G. Zeng, P. Xu, Y. Zhao, Metal-organic framework-derived nanomaterials in environment related fields: Fundamentals, properties and applications. Coord. Chem. Rev. 429 (2021) 213618.

[3] W. J. Stark, P. R. Stoessel, Wohlleben, W., A. J. C. S. R. Hafner, Industrial applications of nanoparticles. Chem. Soc. Rev. 4 4 (16) (2015) 5793-5805.

[4] Park, S. E., Chang, J. S., Hwang, Y. K., Kim, D. S., Jhung, S. H., Hwang, J. S. Supramolecular interactions and morphology control in microwave synthesis of nanoporous materials, Catal. Surv. Asia. 8(2) (2004) 91-110.

[5] X. Sun, Y. Li, Colloidal carbon spheres and their core/shell structures with noble‐metal nanoparticles. Angew. Chem. Int. Ed. 116 (5) (2004) 607-611.

[6] I. Y. Jeon, J. B. Baek, Nanocomposites derived from polymers and inorganic nanoparticles. Materials. 3 (6) (2010) 3654-3674.

[7] C. Gao, Z. Guo, J. H. Liu, X. J. Huang, The new age of carbon nanotubes: an updated review of functionalized carbon nanotubes in electrochemical sensors. Nanoscale. 4 (6) (2012) 1948-1963.

[8] K. Liu, Y. Zhao, J. Wang, Q. Xue, G. Zhao, Ag–CoO nanocomposites for gas-phase oxidation of alcohols to aldehydes and ketones: intensified O_2 activation at Ag–CoO interfacial sites. Catal. Sci. Technol. 10 (24) (2020) 8445–8457.

[9] Y. Shi, S. Hou, X. Qiu, B. Zhao, MOFs-based catalysts supported chemical conversion of CO_2. MOFs. (2020) 373-426.

[10] L. X. Zhou, Y. Yang, H. L. Zhu, Y. Q. Zheng, In situ synthesis of Ag/NiO derived from hetero-metallic MOF for supercapacitor application. Chem. Pap. 75 (5) (2021)1795-1807.

[11] K. Shah, Biodegradation of azo dye compounds. IRJBB, 1 (2) (2014) 5-13.

[12] M. B. Pavithra, A study on the historical evolution of tanneries in India and its tribulations. J. Contemp. Hist. (2019) 461.

[13] A. Khan, A. Roy, S. Bhasin, T. B. Emran, A. Khusro, A. Eftekhari, F. Karimi, Nanomaterials: An alternative source for biodegradation of toxic dyes. Food Chem. Toxicol. (2022) 112996.

[14] A. M. Elgarahy, K. Z. Elwakeel, S. H. Mohammad, G. A. Elshoubaky, A critical review of biosorption of dyes, heavy metals and metalloids from wastewater as an efficient and green process. Clean Engine. Technol. 4, (2021) 100209.

[15] A. Roy, H. A. Murthy, H. M. Ahmed, M. N. Islam, R. Prasad, Phytogenic synthesis of metal/metal oxide nanoparticles for degradation of dyes. J. Renew. Mater. 10 (7) (2022) 1911.

[16] H. Hayati, A. Mesbahi, M. Nazarpoor, Monte Carlo modeling of a conventional X-ray computed tomography scanner for gel dosimetry purposes. Radiol. Phys. Technol. 9 (1) (2016) 37-43.

[17] Y. Fu, L. Qin, D. Huang, G. Zeng, C. Lai, B. Li, X. Wen, Chitosan functionalized activated coke for Au nanoparticles anchoring: Green synthesis and catalytic activities in hydrogenation of nitrophenols and azo dyes. Appl. Catal. B. 255 (2019) 117740.

[18] Z. Yang, X. Tong, J. Feng, S. He, M. Fu, X. Niu, X. Feng, Flower-like BiOBr/UiO-66-NH_2 nanosphere with improved photocatalytic property for norfloxacin removal. Chemosphere, 220 (2019) 98-106.

[19] C. Dong, J. Ji, Z. Yang, Y. Xiao, M. Xing, J. Zhang, Research progress of photocatalysis based on highly dispersed titanium in mesoporous SiO_2. Chin. Chem. Lett. 30 (4) (2019) 853-862.

[20] D. Wang, F. Jia, H. Wang, F. Chen, Y. Fang, W. Dong, X. Yuan, Simultaneously efficient adsorption and photocatalytic degradation of tetracycline by Fe-based MOFs. J. Colloid Interface Sci. 519 (2018) 273-284.

[21] J. M. D. Dikdim, Y. Gong, G. B. Noumi, J. M. Sieliechi, X. Zhao, N. Ma, J. B. Tchatchueng, Peroxymonosulfate improved photocatalytic degradation of atrazine by activated carbon/graphitic carbon nitride composite under visible light irradiation. Chemosphere. 217 (2019) 833-842.

[22] K. Ithisuphalap, H. Zhang, L. Guo, Q. Yang, H. Yang, G. Wu, Photocatalysis and photoelectrocatalysis methods of nitrogen reduction for sustainable ammonia synthesis. Small Methods. 3 (6) (2019) 180035.

[23] P. Rajasulochana, V. Preethy, Comparison on efficiency of various techniques in treatment of waste and sewage water–A comprehensive review. Resource-Efficient Technologies. 2 (4) (2016) 175-184.

[24] M. C. Collivignarelli, A. Abbà, M. C. Miino, S. Damiani, Treatments for color removal from wastewater: State of the art. J. Environ. Manage. 236 (2019) 727-745.

[25] V. Katheresan, J. Kansedo, S. Y. Lau, Efficiency of various recent wastewater dye removal methods: A review. J. Environ. Chem. Eng. 6 (4) (2018) 4676-4697.

[26] A. T. Babu, R. Antony, Green synthesis of silver doped nano metal oxides of zinc copper for antibacterial properties, adsorption, catalytic hydrogenation & photodegradation of aromatics. J. Environ. Chem. Eng. 7 (1) (2019) 102840.

[27] G. Manjari, S. Saran, S. Radhakrishanan, P. Rameshkumar, A. Pandikumar, S. P. Devipriya, Facile green synthesis of Ag–Cu decorated ZnO nanocomposite for effective removal of toxic organic compounds and an efficient detection of nitrite ions. J. Environ. Manage. 262 (2020) 110282.

[28] Y. Zuo, L. Li, X. Huang, G. Li, Ce 0.9 Fe 0.1 O 1.97/Ag: a cheaper inverse catalyst with excellent oxygen storage capacity and improved activity towards CO oxidation. Catal. Sci. Technol. 4 (2) (2014) 402-410.

[29] K. S. Krishna, S. Maity, K. K. R. Datta, Carbon spheres assisted synthesis of porous oxides with foam-like architecture. J. Nanosci. Nanotechnol. 13 (4) (2013) 3121-3126.

[30] G. A. Ashraf, R. T. Rasool, M. Hassan, L. Zhang, H. Guo, Heterogeneous catalytic activation of BaCu-based M-hexaferrite nanoparticles for methylene blue degradation under photo-Fenton-like system. Mol. Catal. 505 (2021) 111501.

[31] R. Dou, H. Cheng, J. Ma, Y. Qin, Y. Kong, S. Komarneni, Catalytic degradation of methylene blue through activation of bisulfite with CoO nanoparticles. Sep. Purif. Technol. 239 (2020) 116561.

[32] J. Lian, D. Yin, S. Zhao, X. Zhu, Q. Liu, X. Zhang, X. Zhang, Core-shell structured Ag-CoO nanoparticles with superior peroxidase-like activity for colorimetric sensing hydrogen peroxide and o-phenylenediamine. Colloid surf. A-physicochem. eng. Asp. 603 (2020) 125283.

[33] F. Mei, J. Zhang, C. Liang, K. Dai, Fabrication of novel CoO/porous graphitic carbon nitride S-scheme heterojunction for efficient CO_2 photoreduction. Mater. Lett. 282 (2021) 128722.

[34] H. Karimi-Maleh, B. G. Kumar, S. Rajendran, J. Qin, S. Vadivel, D. Durgalakshmi, F. Karimi, Tuning of metal oxides photocatalytic performance using Ag nanoparticles integration. J. Mol. Liq. 314 (2020) 113588.

[35] F. P. Fato, D. W. Li, L. J. Zhao, K. Qiu, Y. T. Long, Simultaneous removal of multiple heavy metal ions from river water using ultrafine mesoporous magnetite nanoparticles. ACS omega, 4 (4) (2019) 7543-7549.

[36] R. Fatima, M. F. Warsi, M. I. Sarwar, I. Shakir, P. O. Agboola, M. F. A. Aboud, S. Zulfiqar, Synthesis and Characterization of Hetero-metallic Oxides-Reduced Graphene Oxide Nanocomposites for Photocatalytic Applications. Ceram. Int. 47 (6) (2021) 7642-7652.